

# Control of wavefront propagation in two-dimensional bistable system

Takashi ISOSHIMA

Nano Medical Engineering Laboratory, RIKEN  
2-1 Hirosawa, Wako, Saitama 351-0198, Japan  
Email: isoshima@riken.jp

**Abstract**– A spatial expanse of bistable system can support traveling wavefront which is an interface between different stable states (ex. “on” and “off” states). We investigate a two-dimensional optical bistable device (2DOBD) and its application to maze exploration. We have reported that such a device can present not only extension of “on” state, but also reduction mode in which “on” state area retreats from dead-end path. In this paper we report controllability of wavefront propagation properties by light intensity, which is an important advantage of this device for realization of high functionality in natural computing.

## 1. Introduction

A bistable system with a spatial expanse can keep two stable states (here we assign the terms “on” and “off” to these states) simultaneously at different locations. [1]. The interface between “on” and “off” area, here we call it “wavefront”, can spatially propagate. We are interested in such wavefront propagation to utilize for natural computing. Natural computing is a novel information processing scheme utilizing dynamics of various natural phenomena. Natural computing is attracting attentions as an alternative to silicon-based digital computing. Maze exploration is one of popular applications of natural computing. For example, Belousov-Zhabotinsky (BZ) excitable reaction wave [2], self-propelling oil droplet [3], movement of true slime mold [4] and many other natural phenomena have been reported to solve mazes. In this work, we introduce a two-dimensional thermo-optical bistable device as a system for wavefront propagation, to realize maze exploration.

In our device, optical bistability is realized through positive feedback between heat generated by photoabsorption and temperature-dependent optical absorption. Under irradiation of bias light at an intensity in the bistable (hysteresis) region, the whole area of the device can stay at “off” (low photoabsorption) state without any perturbation. Once the light intensity is increased above the turn-on threshold at one location, the medium is locally triggered and transit to high photoabsorption (“on”) state. The turn-on wavefront expands two-dimensionally through thermal diffusion. Maze pattern can be easily defined by patterned light irradiation, and exploration can be started by irradiating strong trigger light at the start point of the maze.

The device structure we investigate in this work is shown in Fig.1. It is composed of a top cover, a liquid

crystal layer, and a black light-absorbing bottom substrate. The bottom black substrate absorbs light transmitted through the liquid crystal layer, converting light to heat. Temperature-dependent optical transmission change is realized by phase transition of liquid crystal. In this work, we employ 4-Cyano-4'-pentylbiphenyl (5CB) showing nematic-isotropic phase transition at about  $T_{PT} = 35$  °C. At a temperature lower than  $T_{PT}$ , optical transmission is low due to light scattering. If the temperature raises above  $T_{PT}$  the liquid crystal transit to isotropic phase and becomes transparent. When the device is irradiated with a weak light, transmitted small fraction of light is absorbed by the bottom black layer and the temperature of the device increases slightly. Increase of the light intensity causes increase of the temperature, and at the phase transition temperature a positive feedback starts: increase of transmission by phase transition results in increase of heat generation and temperature, which causes further increase of transmission. Finally the device transit to the high transmission (on) state (turn-on transition). When the light intensity is reduced, transition to the low transmission (off) state occurs at a lower light intensity than in the turn-on transition, showing a hysteresis character. With a spatial expanse, the device can provide wavefront propagation, which can be utilized for natural computing including maze exploration, as described above.

In this paper, we describe numerical simulation of the device, to demonstrate exploration of Steinbock's maze pattern [2]. Wavefront reduction mode is introduced, in which wavefront retreats from dead-end paths. Wavefront propagation property is also examined, showing flexible controllability of wavefront velocity.

## 2. Numerical Simulation Method



Figure 1: Schematic cross-sectional diagram of an opto-thermal bistable device based on nematic-isotropic phase transition of a liquid crystal. The light irradiated from top transmits through the liquid crystal layer and is absorbed in the black substrate to be converted to heat. The liquid crystal presents lower optical transmission due to optical scattering at low temperature in nematic phase (shown in gray), while it shows higher transmission at higher temperature in isotropic phase (shown in white). The wavefront, interface between gray and white area, can propagate laterally.

The opto-thermal bistable device with a spatial expanse can be modeled by a thermal diffusion equation as follows: [5,6]

$$\frac{\partial T}{\partial t} = \Delta T + \sigma - \rho \quad (1)$$

$$\sigma = A(T) I \quad (2)$$

$$\rho = \alpha T \quad (3)$$

where  $t$  is the time,  $T$  the temperature,  $\sigma$  the generated heat,  $\rho$  the heat loss to outside of the device,  $A$  the temperature-dependent optical absorption,  $I$  the incident light intensity, and  $\alpha$  the heat dissipation coefficient (heat resistance) [6]. Nonlinearity necessary for bistability is included in the term  $A(T)$ .

Time-dependent 3-D numerical simulation was performed by the finite element method using FreeFEM++ software [7]. Device structure shown in Fig.1 was simulated. Acrylic polymer was assumed as the material of the substrate and the top cover. Bottom of the substrate contacted to a hot plate at constant temperature of 30 °C, and the top cover and side wall of the device were exposed to air at 25 °C. Thicknesses of the top cover, 5CB layer, black layer, and substrate were 0.2, 0.1, 0.02, and 1.0 mm, respectively (here the black bottom substrate in Fig.1 is separated into thin black layer and substrate for convenience of calculation). Optical absorption of the black layer was 100 %. Thermal diffusion constant of acrylic polymer and 5CB is 0.92 and 1.0 [ $10^{-3} \text{ cm}^2 \text{ s}^{-1}$ ], respectively. Heat dissipation constant (heat resistance) at the boundary of the devices is  $0.92 \times 10^{-2} [\text{W } ^\circ\text{C}^{-1}]$ . Division number in vertical direction was 140, and in lateral direction, division number was selected so that the element size is 0.05 mm. Time step was 5 sec for maze exploration simulation and 2 sec for investigation on wavefront velocity. Temperature-dependent transmission of 5CB layer was assumed to be 0.5 at lower than 35 °C, 1.0 at higher than 37 °C, and linearly increasing from 0.5 to 1.0 in the temperature range of 35 to 37 °C. Light intensity used in maze exploration was 0.22 and 0.07 W/cm<sup>2</sup> at the path and the wall area of the maze, respectively. Trigger light intensity was 0.4 W/cm<sup>2</sup>. Steinbock's maze pattern [2] was used, with a width of paths and walls of 3 mm. Total size of the maze was 57×51 mm. Determination of width is described in the following chapter.

For investigation of wavefront propagation velocity, another maze pattern was designed (see inset of Fig.4). The dead-end path at the center is the test path. Width of paths and walls was 3 mm, and total size of the maze was 21×36 mm. Time-dependent finite element method calculation was performed with a time step of 2 sec. For the first 200 sec, an initial maze pattern was irradiated to achieve stationary "on" area, then a test maze pattern was irradiated for up to 3600 sec. For investigation of the reduction mode, the pattern shown as the inset of Fig.4 was used as the initial and test maze patterns. For the extension mode, the pattern without the center finger was used as the initial maze pattern, and the pattern shown as the inset of Fig.4 was used as the test one. Position of the wavefront at the end of the center finger was obtained as the position where the temperature is the phase transition

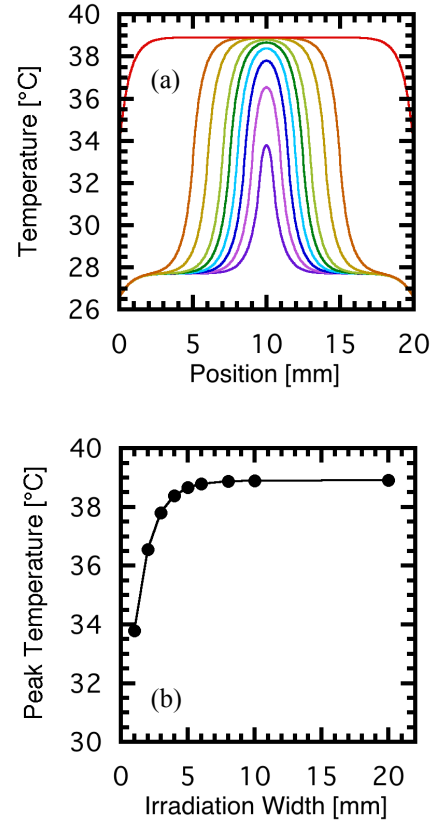


Figure 2: (a) Temperature distribution of the liquid crystal layer at equilibrium condition. Device width is 20 mm and light intensity of the irradiated path area is 0.2 W/cm<sup>2</sup>. Each line represents temperature distribution for different light irradiation width of (from bottom to top) 1, 2, 3, 4, 5, 6, 8, 10, and 20 mm. (b) Highest temperature for each distribution in (a) as a function of light irradiation width.

temperature, and was plotted as a function of time. Wavefront propagation velocity was obtained as the slope of the plot.

### 3. Results and Discussions

#### 3.1. Path width for maze exploration

To design light irradiation pattern of a maze for a practical device, it is necessary to determine path width. Narrower width is preferable because the device size becomes smaller. If the device size is same, larger and more complex maze can be realized if the path width is narrower. Moreover, smaller device size results in shorter time for wavefront propagation from the start to the goal of the maze, if wavefront velocity is same. However, thermal diffusion prevents high contrast in temperature distribution, if the path width is too narrow. This is graphically described in Fig.2 (a), stationary temperature distribution at various path width. In Fig. 2 (b), peak temperature of each distribution is plotted as a function of width. In narrower path width of 1 and 2 mm, peak temperature is significantly reduced from that in wider

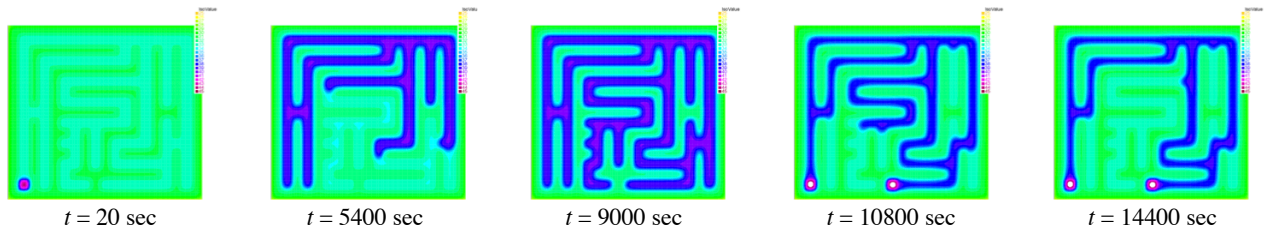


Figure 3: Numerical simulation of exploration of Steinbock's maze pattern. Snapshots at  $t = 20$  (start), 5400, and 9000 sec present temporal evolution of "on" state area (blue) in the extension mode. At  $t=9000$  sec, all maze paths are explored, and the light intensity at the paths is reduced to enter the reduction mode. Snapshot at  $t = 10800$  sec shows "on" state area retreating from the dead-end paths, and finally at  $t = 14400$  sec, only the connected paths (solution of the maze) remains in "on" state, showing completion of maze exploration. In the snapshot images, color shows temperature: green stands for  $30\text{ }^{\circ}\text{C}$ , light blue  $34\text{ }^{\circ}\text{C}$  where is the path region in "off" state, dark blue  $38^{\circ}\text{C}$  where is the path region in "on" state, red-purple  $45^{\circ}\text{C}$  for trigger, white  $>45^{\circ}\text{C}$  in the reduction mode corresponding start and goal points where high light intensity same as the trigger is applied to keep the dead-end start and goal points in "on" state.

paths. Considering these results, we decided to use the path width of 3 mm for the following simulation.

### 3.2. Maze exploration

Figure 3 shows temporal evolution of temperature distribution at the liquid crystal layer of the device, in exploration of Steinbock's maze pattern. From  $t = 1$  to 30 sec, trigger light at intensity of  $0.4\text{ W/cm}^2$  is irradiated at the bottom-left start point of the maze. The snapshot at  $t = 20$  sec shows temperature distribution during the trigger, showing significant increase of temperature at the start point. Temperature of the paths of the maze, shown in light blue in the snapshots, is about  $34\text{ }^{\circ}\text{C}$ , higher than that of the walls (about  $30\text{ }^{\circ}\text{C}$ ) but lower than the phase transition temperature, thus staying in "off" state. The "turn-on" wavefront propagates through the paths even after the trigger is turned off at  $t = 30$  sec, exploring the maze ( $t = 5400$  sec). At  $t = 9000$  sec, wavefronts reach all path ends, and all the path is in "on" state. In this simulation, light intensity at the wall area  $I_{\text{wall}}$  is  $0.07\text{ W/cm}^2$ . If  $I_{\text{wall}}$  is 0 or small value, the intensity at the path area must be increased to be in bistable region, but such a high intensity causes spontaneous turn-on without trigger or wavefront propagation at a three-paths connection (branch).

At the moment of full extension at  $t = 9000$  sec, intensity of light irradiated to the paths  $I_{\text{path}}$  is reduced from  $0.220$  to  $0.205\text{ W/cm}^2$  to enter the reduction mode, except for the start and goal points where light intensity is increased to  $0.4\text{ W/cm}^2$  to keep these points "on". In the reduction mode, the dead end point of each path turns "off" while the connected points remain in "on" state, because a dead end point faces more of cooler surrounding area than a connected point. Simply considering four neighbor pixels, a dead end point is surrounded by three low-temperature pixels and one high-temperature "on" pixel, while a connected point is surrounded by two low-temperature pixels (walls) and two high-temperature "on" pixels. This results in difference of heat flow balance, causing "turn-off" only in a dead-end point. Therefore, if the light intensity is too low, not only the dead-end points but also all connected path can be turned "off". The intensity above was determined after

some trial and errors. In the simulation, retreat of the "on" area is observed in the snapshot at  $t = 10800$  sec., and finally retreat from all dead-end paths completes at  $t = 14400$  sec. At this moment, only the paths connecting the start and goal points remain in "on" state, thus completion of the maze exploration. The solution is visualized as the "on" area of the device.

This maze exploration method can find all connected paths even if there exist more than one, but cannot find the shortest path in principle. In general, maze exploration methods in natural computing can be categorized in two types: one is exploration with some kind of potential gradient, and the other without potential gradient. Our method belongs to the latter, as well as the method using BZ reaction wave [2]. Self-propelling oil droplet method [3] belongs to the former category, since the oil droplet traces pH gradient toward the goal with acid. The former can find the shortest path by tracing the most steep gradient of the potential, but finding all solutions (if more than one exist) is not guaranteed. Another possible problem in the former is scalability: if the maze becomes large and complex, the potential gradient gets smaller, and trace will be harder. The latter has opposite advantage and disadvantage: all solutions can be found, but finding the shortest one is not guaranteed (some post-processing is necessary); no problem in scalability and solutions can be found even for a larger and complex maze. True slime mold [4] is a special case: in extension mode it extends without food, so there is no potential gradient; in reduction mode, foods are placed at start and end points, and therefore some nutrient concentration gradient can be formed within the true slime mold, resulting in finding the shortest path. However, this mechanism is not well understood yet.

### 3.3. Wavefront propagation property

Wavefront propagation velocity was calculated at various light intensity. Figure 4 shows wavefront velocity as a function of  $I_{\text{path}}$ , the light intensity at the path. Light intensity at the wall  $I_{\text{wall}}$  is  $0.07\text{ W/cm}^2$ . A positive value of wavefront velocity stands for extension of "on" area (forward propagation of wavefront), while a negative value stands for retreat (backward propagation of

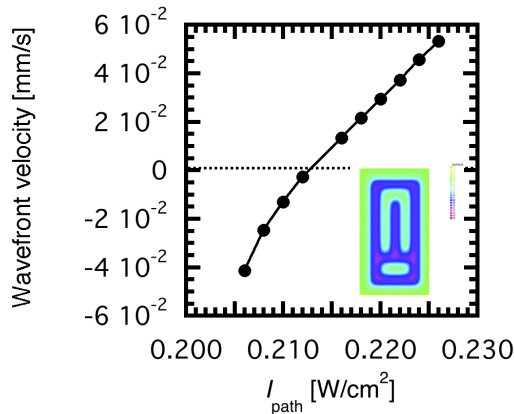


Figure 4: Wavefront velocity calculated at various light intensity. Positive value stands for extension and negative value reduction of wavefront. Path width is 3 mm, and the light intensity at the wall area  $I_{\text{wall}}$  is 0.07 (black) W/cm<sup>2</sup>.  $I_{\text{path}}$  stands for the light intensity at the path area. The inset shows the maze pattern for wavefront velocity calculation. The dead-end path at the center is the test path.

wavefront). The wavefront velocity increases almost linearly with  $I_{\text{path}}$ , from negative value (reduction mode) to positive (extension mode). Therefore, control of wavefront propagation velocity is easily achieved by control of  $I_{\text{path}}$ , although we also have to consider possibility of spontaneous turn-on at three- or four-paths connection area at too high  $I_{\text{path}}$ , and of spontaneous turn-off at the connected path in the reduction mode at too low  $I_{\text{path}}$ . Investigation of the phase diagram of operation condition is now in progress, and will be reported separately.

#### 4. Concluding Remarks

In this paper, we have demonstrated by the finite element method calculation that a maze can be explored by an experimentally feasible opto-thermal bistable device with a spatial expanse. In this device, wavefront propagation property can be easily controlled by light intensity. Direction of wavefront propagation can be controlled: in extension mode, the "on" state area extends, and in reduction mode, it retreats from the dead-end path if the light intensity is suitably reduced. Temperature distribution was calculated for various path width and 3 mm is found to be practical minimum width for this device structure and materials.

Exploration of Steinbock's maze pattern has been demonstrated utilizing the extension and reduction modes: firstly "on" state area extends to all the paths in extension mode, then turned to reduction mode where the "on" state area retreated only from the dead-end paths, and finally all paths connecting the start and stop points remains in "on" state. Such a reduction mode has been reported only for the true slime mold [4], but not for other natural computing methods. Wavefront propagation velocity was examined as a function of light intensity, showing almost linear dependence.

Controllable wavefront propagation in our two-dimensional optical bistable device can be a powerful tool in natural computing. Experimental investigation is in progress, and will be reported separately.

#### Acknowledgments

This work is financially supported by Japan Society for the Promotion of Science (Grant-in-Aid for Scientific Research No.26540129).

#### References

- [1] J. D. Murray, "Mathematical Biology I: An Introduction - Third Edition," Chapter 13, Springer Science+Business Media, New York, 2001.
- [2] O. Steinbock, Á. Tóth, K. Showalter, "Navigating Complex Labyrinths: Optimal Paths from Chemical Waves", *Science*, Vol.267, p.868, 1995.
- [3] I. Lagzi, S. Soh, P. J. Wesson, K. P. Browne, B. A. Grzybowski, "Maze Solving by Chemotactic Droplets", *J. Am. Chem. Soc.*, Vol.132, p.1198, 2010.
- [4] T. Nakagaki, H. Yamada, Á Tóth, "Maze-solving by an amoeboid organism", *Nature*, Vol.407, p.470, 2000.
- [5] Y. Okabayashi, T. Isoshima, E. Nameda, S. Kim, M. Hara, "Two-Dimensional Nonlinear Fabry-Perot Interferometer: An Unconventional Computing Substrate for Maze Exploration and Logic Gate Operation.," *Int. J. Nanotech. Mol. Comp.*, Vol.3, p.13, 2011.
- [6] T. Isoshima and Y. Ito, "Two-dimensional optical bistable device with external feedback for pulse propagation and spatio-temporal instability", *Proc.NOLTA2014*, p.625, 2014.
- [7] Université Pierre et Marie Curie and Laboratoire Jacques-Louis Lions, *FreeFEM++*, <http://www.freefem.org/ff++/>